EXPERIMENTAL PERFORMANCE ANALYSIS OF AN AMMONIA-WATER DIFFUSION ABSORPTION REFRIGERATION CYCLE

Najjaran A., Freeman J., Ramos A., Markides C.N.*
*Author for correspondence
Department of Chemical Engineering,
Imperial College London,
London, SW7 2AZ,
United Kingdom,
E-mail: c.markides@imperial.ac.uk

ABSTRACT

Absorption-refrigeration systems are emerging as an important technology for the utilisation of low- and medium-temperature thermal-energy, such as renewable- and waste-heat sources, as a means of addressing the quickly accelerating global demand for cooling. In particular, systems based on the ammonia-water diffusion absorption refrigeration (DAR) cycle are of particular interest for cooling in off-grid regions and in developing countries due to their low capital costs, low maintenance requirements and unique design in which the requirement for an electrically driven pump is omitted. In this work, a detailed experimental evaluation is undertaken of a DAR unit with a nominal cooling capacity of 120 W. Electrical cartridge heaters are used to provide the thermal input which can be varied in the range 300-700 W at generator temperatures of 150-200 °C. Heating is also supplied to the air inside an insulated cold-box constructed around the evaporator which, by counter-acting the cooling effect, allows the cooling output to be measured indirectly. Tests are performed with the DAR system charged to default factory settings (23.8 bar and an ammonia concentration of 30% by wt.). The cooling output obtained is in the range 79-104 W, corresponding to a coefficient of performance (COP) in the range 0.11-0.26. Results are compared to performance calculations from a steady-state system model, showing acceptable agreement for a model of this fidelity. Temperature measurements at various points in the system are used to provide further verification of the model assumptions. In particular, the temperatures measured in the condenser are used to evaluate the degree of sub-cooling and the effectiveness of the rectification process; while the air temperature and flow regime in contact with the evaporator are found to have a non-negligible effect on the predictions of the cooling output and the COP of the system.

NOMENCLATURE

Variables

c_p	Specific heat capacity, J/(kg K)
h	Specific enthalpy, J/kg
$\dot{m}$	Mass flow rate, kg/s
p	Pressure, bar
$\dot{Q}$	Heating or cooling rate, W
T	Temperature, °C
x	Molar fraction of ammonia in liquid phase
y	Molar fraction of ammonia in gas phase
ε	Effectiveness

Subscripts

abs	Absorber
cond	Condenser
evap	Evaporator
gen	Generator
ig	Inert gas
LHX	Liquid heat exchanger
GHX	Gas heat exchanger
rect	Rectifier

INTRODUCTION

The worldwide demand for cooling is a major consideration for future energy policy, exacerbated by increased living standards in developing and emerging-market regions. By 2050, it is expected that energy consumption for space cooling will double, with more than 80% of the growth occurring in non-OECD countries [1]. Thermally-driven absorption-refrigeration systems are one alternative to vapour-compression systems in which some or all of the energy to drive the cooling process is provided by a low- or medium-temperature heat source such as solar, geothermal or waste heat. Absorption-refrigeration cycles differ from vapour-compression cycles in the way that the refrigerant is returned from a vapour to a liquid phase. In absorption cycles the vapour is absorbed into a second fluid component (an *absorbent*) with a higher boiling point, thereby omitting the requirement for a compressor, however, most absorption-refrigeration systems require a small amount of electrical energy to drive a circulation pump. The most common refrigerant-absorbent working fluid pairs are NH_3-H_2O and H_2O-LiBr (it should be noted that in the former, water is the refrigerant while in the latter it is the absorbent).

The diffusion absorption refrigeration (DAR) system, originally developed by von Platen and Munters [2], is a technology that requires no electrical energy input, and can be manufactured on small scales (< 0.5 kW cooling). As such, the technology shows strong potential for use in rural communities in developing regions, where crop and vaccine supply-chain management require low cost, distributed cooling solutions [3]. The main feature of the DAR system is the use of an inert gas to provide a low partial pressure atmosphere in the evaporator and a solution bubble-pump coupled to the generator in order to use the thermal input power to drive the fluid circulation. The conventional system uses ammonia as the refrigerant, water as the absorbent, and hydrogen as the inert gas.

A DAR system is shown in Fig. 1. In the generator, the refrigerant-rich solution is heated (1-2) forming vapour bubbles that are lifted through the bubble tube with a small amount of liquid (2-3,4). Ammonia refrigerant is separated from the water absorbent in the rectifier (5) which flows downwards in the solution heat exchanger and is then sent to absorber (8). The refrigerant vapour proceeds to the condenser where it condenses (6-7) releasing heat to the surroundings. The resulting liquid is pre-cooled in the gas heat exchanger on its way to the evaporator, which is loaded with inert gas (hydrogen); thus the refrigerant's partial pressure drops and low-temperature evaporation begins (9-10), producing the refrigeration effect. The refrigerant vapour then enters the absorber where the refrigerant is captured by the absorbent, releasing heat to the surroundings. The inert gas is not absorbed and, being less dense the refrigerant, rises back to the evaporator in the gas heat exchanger.

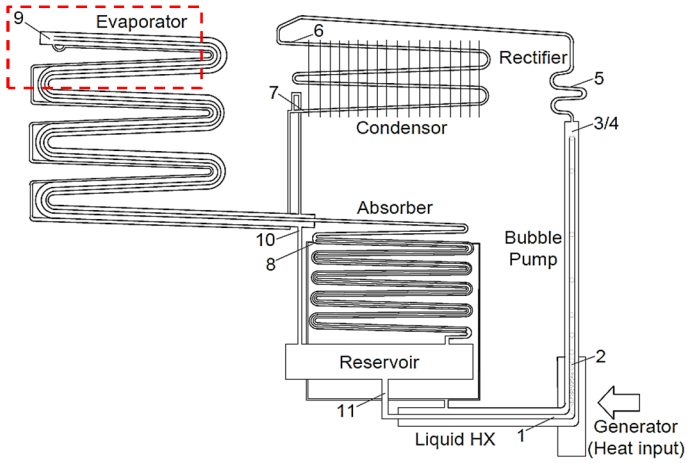

State points			
1.	Generator inlet	6.	Condenser inlet
2.	Generator outlet	7.	Condenser outlet
3.	Bubble pump outlet (liquid)	8.	Absorber, liquid inlet
4.	Bubble pump outlet (vapour)	9.	Evaporator inlet
5.	Rectifier	10.	Evaporator outlet
		11.	Reservoir

Figure 1. Schematic of the DAR system used in the present work with key state points. The box around the top of the evaporator indicates the part of the system shown in Fig. 2.

The main advantage of DAR systems arises from their low capital costs (~0.5 £/W), despite coefficients of performance (COP) typically lower than 0.4, compared to 0.6 for single-effect absorption chillers, and ~1.0 for double-effect systems [4]. Recently a renewed interest has been shown in this technology for coupling with a wide range of heat sources including solar collectors [5,6]. Although a small number of thermodynamic models have been developed in the literature, there is a further need for experimental validation of these models across a wide range of operating conditions. In this paper, we perform an experimental analysis of a laboratory DAR system operating in steady state over a range of thermal input powers. Attention will be given to the performance of the evaporator and condenser, and how their performance is affected by the increased carry-over of water from the rectifier at higher input thermal powers.

EXPERIMENTAL METHODS

The present experimental analysis was performed on a laboratory DAR system, of nominal cooling capacity 120 W, with a thermal input provided at the generator by electrical cartridge heaters delivering a maximum heating capacity of 700 W. The cartridge heaters were inserted into an aluminium heat exchanger block clamped around the generator tube and controlled using an AC autotransformer to manually vary the generator heating load. The generator and bubble pump were both insulated to minimise heat losses to the environment.

An insulated cold-box was also constructed around the evaporator using 30-mm thick insulation boards with a thermal conductivity of 0.021 W/mK. The inner dimensions of the cold-box space are 800×450×200 mm, yielding a volume of 0.072 m^3 and a surface area of 1.22 m^2. For the experimental results in the present study, the internal air temperature in the cold box was maintained at a temperature approximately equal to the ambient air condition in the laboratory in order to negate heat losses from the cooling capacity calculation. To control the air temperature in the cold space, a small electric air heater was used with a fan to circulate air and provide a more uniform temperature inside the cold box (monitored by thermocouples positioned at various locations). The air heater and fan were also manually controlled using a variable transformer.

The electrical heating power provided to the generator and the cold-box was monitored independently using two Rodhe and Schwarz AC power analyser units. All temperatures on the DAR system were measured using K-type thermocouples and measurements were logged automatically at an interval of 1 s. Measurements were performed at generator heat input intervals of approximately 50 W over the range 300-700 W.

Temperatures were measured at various points on the DAR unit as indicated in Fig. 1, which are also key representative state points used in the thermodynamic model. For the temperature measurement at the evaporator inlet (State 9), a large variation in temperature was observed close to the mixing point between the refrigerant and inert gas flows. Thus in the present work, temperatures were measured at four locations along the top of the evaporator, shown in Fig. 2.

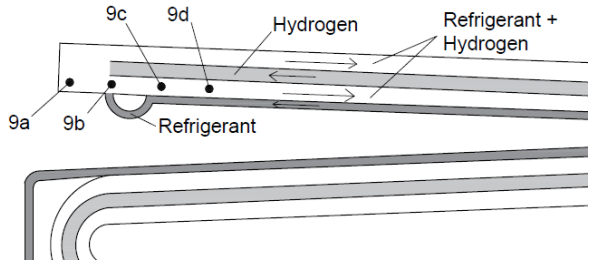

Figure 2. Zoomed-in schematic showing the inlet/mixing section of the DAR evaporator.

THERMODYNAMIC MODEL

The thermodynamic model of the DAR system is based on the equations of Starace & De Pascalis [7]. The main energy balance equations are summarised below. Starting with the generator and bubble pump, the total enthalpy increase imparted to the ammonia-water solution is equal to the thermal energy supplied at the generator:

$$\dot{Q}_{\text{gen}} = \dot{m}_3 h_3 + \dot{m}_4 h_4 - \dot{m}_1 h_1 \,. \quad (1)$$

It is assumed that with sufficient insulation, heat losses in the generator and bubble-pump are negligible. Therefore the specific enthalpy of the saturated liquid h_3 and vapour h_4 and is calculated by assuming that $T_2 = T_3 = T_4$.

In the rectifier, near-pure ammonia vapour is separated from the rich solution vapour exiting the bubble pump, also releasing thermal energy to the surroundings:

$$\dot{Q}_{\text{rect}} = \dot{m}_5 h_5 + \dot{m}_6 h_6 - \dot{m}_4 h_4 \,, \quad (2)$$

where $\dot{m}_6$ is the mass flow-rate of vapour proceeding to the condenser. In the condenser, heat is rejected as the ammonia refrigerant (plus a small residual water fraction) is condensed:

$$\dot{Q}_{\text{cond}} = \dot{m}_6 (h_7 - h_6) \,. \quad (3)$$

The liquid refrigerant flow-rate proceeding to the evaporator is equal to the that leaving the condenser, $\dot{m}_6 = \dot{m}_7 = \dot{m}_9$. The energy balance for the evaporator considers both the pre-cooling and evaporation processes, and also the mass-flows of refrigerant and inert gas:

$$\dot{Q}_{\text{evap}} = \dot{m}_9 (h_{10} - h_7) + \dot{m}_{\text{ig}} \left(h_{10.\text{ig}} - h_{8.\text{ig}}\right) \,. \quad (4)$$

In the absorber, ammonia mixed with inert gas is introduced from the bottom (State 10 and 10,ig) via the reservoir, while weak solution is introduced at the top (State 8). Ammonia is absorbed into the weak solution, releasing heat to the surroundings, and the remaining inert gas exits at the top of the absorber (State 10,ig):

$$\dot{Q}_{\text{abs}} = \dot{m}_{11} h_{11} - \dot{m}_{10} h_{10} - \dot{m}_8 h_8 - \dot{m}_{\text{ig}} h_{8.\text{ig}} - \dot{m}_{\text{ig}} h_{10.\text{ig}} \,. \quad (5)$$

Finally, in the liquid heat exchanger thermal energy is transferred from the weak solution separated after the bubble pump to the rich solution leaving the reservoir:

$$\dot{m}_3 h_3 + \dot{m}_5 h_5 - \dot{m}_8 h_8 = \dot{m}_1 (h_1 - h_{11}) \,. \quad (6)$$

It is assumed that no heat losses occur to the surroundings

The COP of the system is the ratio of the cooling output power at the evaporator to the heating input at the generator:

$$\text{COP} = \dot{Q}_{\text{evap}} / \dot{Q}_{\text{gen}} \,, \quad (7)$$

However, a limiting value for the cooling output $\dot{Q}_{\text{evap,max}}$ is also specified based on the maximum cooling that can be delivered to the air stream passing over the evaporator:

$$\dot{Q}_{\text{evap.max}} = \dot{m}_{\text{air}} \, c_{\text{p}} \, \varepsilon \, (T_{\text{amb}} - T_9) \,, \quad (8)$$

where $0 \leq \varepsilon \leq 1$.

To solve the mathematical model described above, it is necessary to calculate various thermodynamic properties of the working fluid (ammonia-water) and of the inert gas (hydrogen), such as enthalpy, temperature, molar concentration and pressure. The vapour-liquid equilibrium properties of the ammonia-water mixture are calculated using the polynomial relations provided by Pátek & Klomfar [8]:

$$T(p,x) = T_0 \sum_i a_i (1-x)^{m_i} \left[\ln\left(\frac{p_0}{p}\right)\right]^{n_i} , \quad (9)$$

$$T(p,y) = T_0 \sum_i a_i (1-x)^{\frac{m_i}{4}} \left[\ln\left(\frac{p_0}{p}\right)\right]^{n_i} , \quad (10)$$

$$y(p,x) = 1 - \exp\left[\ln(1-x) \sum_i a_i \left(\frac{p_0}{p}\right)^{m_i} x^{\frac{n_i}{3}}\right] , \quad (11)$$

$$h_l(T,x) = h_0 \sum_i a_i \left(\frac{T}{T_0} - 1\right)^{m_i} x^{n_i} , \quad (12)$$

$$h_g(T,y) = h_0 \sum_i a_i \left(\frac{T}{T_0} - 1\right)^{m_i} y^{n_i} , \quad (13)$$

where the values of the terms a_i, n_i, m_i are given in Ref. [8].

The DAR system model requires the specification of a number of input parameters, specifically the generator heat input $\dot{Q}_{\text{gen}}$, the total system pressure p_{tot}, and the temperatures T_1, T_2, T_6, and T_9. Based on these inputs, the outputs from the model are the system flow-rates and remaining state-point temperatures, the cooling capacity $\dot{Q}_{\text{evap}}$, and thus also the DAR unit's COP. In the present study, $\dot{Q}_{\text{gen}}$, T_6 and T_9 are provided using direct measurements from the experiments, while p_{tot} = 23.8 bar is assumed from the manufacturer's specifications (it is also assumed that p_{tot} does not increase significantly with generator heat input).

The precise values of T_1 and T_2 meanwhile are more difficult to verify experimentally as they represent the temperatures of the rich solution flowing in the inner tube at the inlet and outlet of the generator, respectively. For the experimental apparatus employed in the present study it was only possible to measure the temperatures at these locations using thermocouples in contact with the wall of the outer tube, through which the return flow of weak solution travels. Thus T_2 was estimated using the assumption of Zohar [9], according to which the rich solution in the inner tube at State 2 is 2 K lower than the temperature measured for the weak solution flowing in the outer tube. Meanwhile, T_1 was estimated by using Eq. 9 and assuming phase equilibrium conditions and an ammonia mole fraction in the fluid reservoir of 0.3 (again, based on information from the manufacturer).

In the present study, the results from the experiments are used to evaluate the following assumptions used to solve the system model in the work by Starace and DePascalis [7]:

I. No sub-cooling occurs in the condenser, hence the fluid exiting at State 7 is a saturated liquid;
II. Refrigerant leaves the evaporator at State 10 as a saturated vapour;
III. The temperature exiting the condenser is assumed equal to the reservoir temperature: $T_7 = T_{11}$;
IV. No thermal losses occur to ambient in the liquid heat exchanger, thus the weak solution entering the reservoir at State 8 cannot be cooled below the temperature of the fluid exiting the reservoir.

RESULTS AND DISCUSSION

Experimental observations

The measured cooling output and COP from the DAR apparatus are plotted over a range of generator heat inputs in Fig. 3. The cooling output is found to be approximately constant at around 100W for heating inputs in the range 400-650 W, beyond which it decreases. It can be considered that under the present conditions the optimal performance point is achieved with a generator input of ~400 W, for which both a high cooling output and a high COP are achieved.

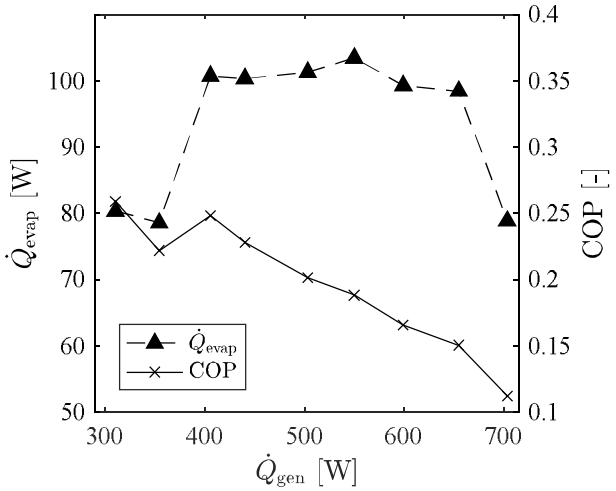

Figure 3. Cooling output and COP of the experimental DAR unit as a function of generator input.

For low heat input conditions, the temperature measured at the condenser inlet T_6 indicates a highly effective separation of water from the rich solution in the rectifier. In Fig. 4, the solution concentration y_6 at the condenser inlet is calculated from using Eq. 10 and an estimated system pressure of p_{tot} = 23.8 bar. For $\dot{Q}_{\mathrm{gen}} \leq$ 500W, estimates of $y_6 >$ 99.8% are obtained.

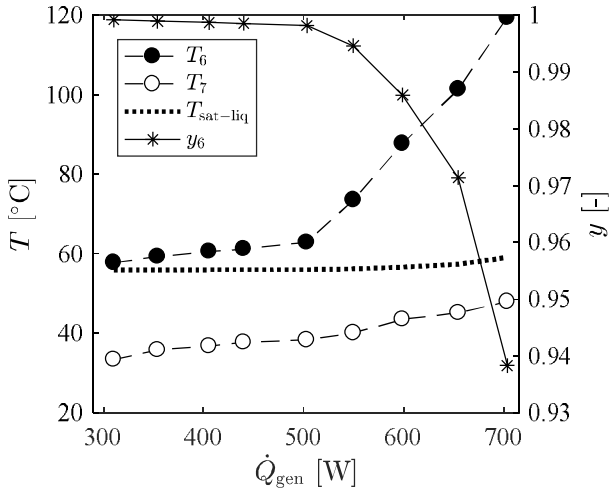

Figure 4. Condenser inlet and outlet temperatures (T_6 and T_7); and estimated molar concentration the condenser inlet (y_6). Also shown is the saturated liquid temperature corresponding to y_6.

The temperature measured at the condenser inlet is observed to increase sharply at generator heat inputs higher than 500 W, indicating an exponential decrease in solution concentration. The dotted line in Fig. 4 shows temperatures expected for a saturated liquid condition at the condenser outlet, based on Eq. 9. The actual temperatures measured at the condenser outlet T_7 are 11-23 K lower than the corresponding saturated liquid temperatures, indicating significant sub-cooling and allowing a revision of Assumption I in the model.

Returning to Fig. 3, the COP predicted by the system model can be seen to be highly dependent on the temperatures in the evaporator (in Fig. 4). An accurate temperature measurement representative of the saturated liquid solution at State 9 was particularly challenging as a large variation in temperature was found to occur between the four measurement points shown in Fig. 2, despite the relatively short spacing interval (~5 cm) between measurement locations. For example, at $\dot{Q}_{\mathrm{gen}}$ = 400W, the temperatures were found to range between 0.1 °C measured at Location 9a to -26.7 °C at Location 9d.

In Fig. 5, the temperature measured closest to the point of refrigerant injection is taken to be the temperature most representative of the saturated liquid refrigerant ($T_9 = T_{9\mathrm{b}}$). The corresponding saturated vapour temperature expected at the outlet of the condenser, according to Assumption II (and assuming also that $y_{10} = x_9 = x_7 = y_6$), is shown by the dotted line. It can be observed that for $\dot{Q}_{\mathrm{gen}} \geq$ 500W, the measured values of the evaporator outlet temperature T_{10} are considerably lower. Furthermore, the measured temperature is close to that of the ambient air (typically maintained at $T_{\mathrm{amb}} \approx$ 24 °C in the tests). It can be concluded that higher generator inputs leading to poorer mixture separation of the solution in the rectifier lead to higher temperatures in the evaporator, which in turn eventually leads to a limitation for the achievable heat transfer with the air medium due to Eq. 8.

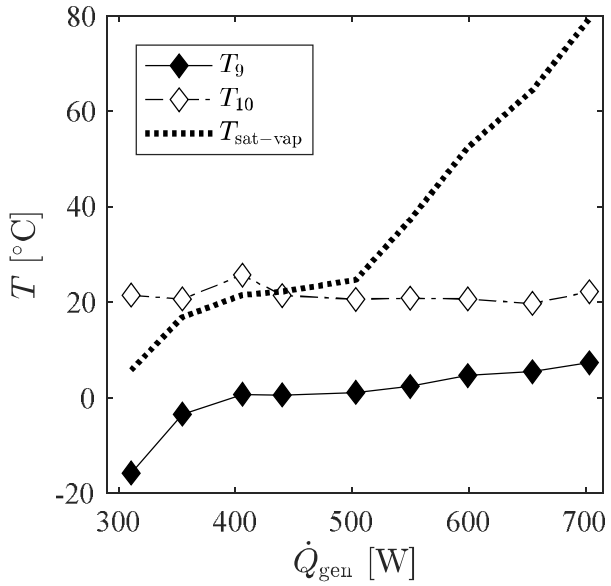

Figure 5. Evaporator inlet and outlet temperatures (T_9 and T_{10}). Also shown is the saturated liquid temperature corresponding to estimated solution concentration and partial pressure.

Finally, the results presented in Fig. 6 may be used to evaluate the validity of Assumptions III and IV. The temperatures T_7 and T_{11} are shown here to be within 2 K of each other across the range of $\dot{Q}_{\text{gen}}$ values between 400-600 W, thus indicating that Assumption III holds reasonably well for this range of operating conditions. With regard to Assumption IV, it can be observed that the inlet temperature of the weak solution introduced at the top of the reservoir T_8 is 4-8 K lower than the temperature measured at the bottom outlet of the reservoir T_{11}, indicating that the weak solution loses some additional thermal energy to the ambient air, as it travels in the outer tube of the concentric tube heat exchanger and then in the connecting tubes that convey the weak solution from the LHX to the entry point at the top of the absorber.

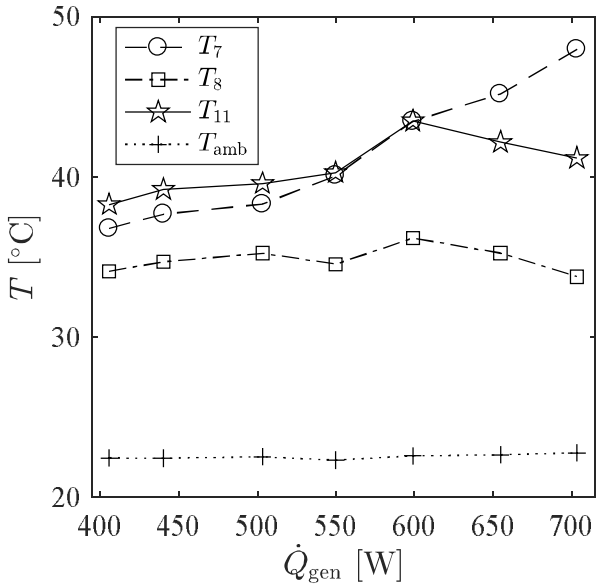

Figure 6. Temperatures at the condenser outlet T_7, absorber inlet T_8, and in the fluid reservoir T_{11}. Also shown is the ambient temperature T_{amb}.

Comparison of experimental results with model predictions

Simulations were performed using two variants of the DAR model to examine the effect of the observed sub-cooling at the exit of the condenser. In the first model variant (Model 1), the temperature at the outlet of the condenser is based on the default assumption of a saturated liquid state at the condenser outlet (Assumption I). In the second variant (Model 2), a varying degree of sub-cooling is assumed based on the experimental measurements in Fig. 4. In both models, an upper limit for the cooling output at the evaporator is included based on the experimental results in Fig. 3, set as $\dot{Q}_{\text{evap,max}}$= 104 W.

Figure 7 shows that for input values of $\dot{Q}_{\text{gen}}$ < 400W, (above which both experimental and numerical results are dominated by the evaporator output limitation), both model variants underestimate the cooling output, however Model 2 shows a significant improvement due to the inclusion of the subcooling at the condenser outlet. Figure 5 indicates that for this range of heat inputs, superheating of the vapour mixture exiting the evaporator at State 10 may be occurring, which may partially account for the under-prediction of the model (which at present assumes a saturated vapour at State 10). A further possible reason for the under-prediction of the cooling output is that additional sub-cooling of the refrigerant after the condenser and prior to the evaporator/GHX may be occurring in the long uninsulated pipe run connecting the components.

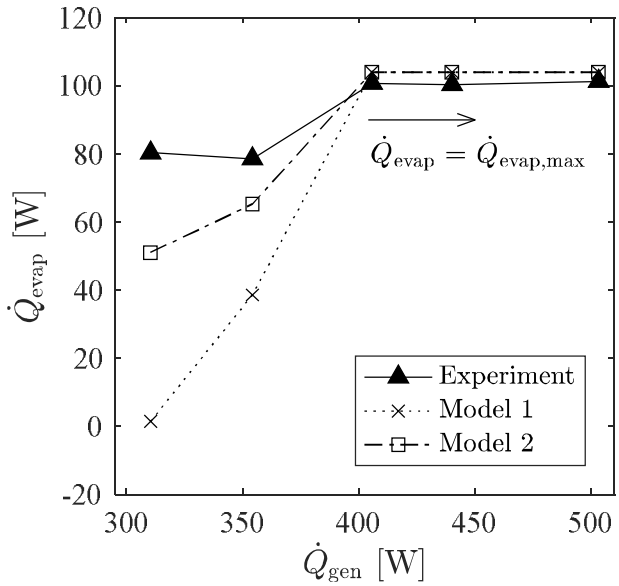

Figure 7. Experimental results compared to two variants of the DAR thermodynamic model: Model 1 (no sub-cooling at condenser outlet) and Model 2 (sub-cooling at condenser outlet).

The above comparison indicates that the present set of experimental data is of some limited use for evaluating the system model, with more results required over a range of operating conditions for which the evaporator performance is not limited due to the external heat transfer process with the air. Thus, an important conclusion is that future tests should be performed over a wider range of air temperatures and flow-rates, with a possible focus on the range of $\dot{Q}_{\text{gen}}$ between 300-400 W for which improved solution separation in the rectifier results in lower temperatures in the evaporator. Detailed heat exchanger sub-models can also be included in the DAR system model to reduce the required number of simplified input assumptions and extend the range over which the system provides a reasonable prediction of performance.

CONCLUSION

A small-scale (nominal cooling capacity 120 W) electrically driven DAR unit was experimentally investigated over a range of generator heat- and temperature-input conditions. Electrical cartridge heaters were used to provide the thermal input which was varied in the range 300-700 W at generator temperatures of 150-200 °C. A cooling output in the range 79-104 W was obtained, corresponding to COP in the range 0.11-0.26.

The assumptions used in a parallel thermodynamic modelling attempt were verified by comparison with the experimental results. The results have been particularly useful for examining the processes of the condenser and evaporator and for evaluating two of the key assumptions of the model; namely that the refrigerant

exits the condenser and evaporator at saturated liquid and saturated vapour conditions, respectively.

Significant liquid sub-cooling in the condenser of 11-23 K was found to occur in the experimental apparatus, across the whole range of investigated conditions. In the evaporator, and at generator heat inputs greater than 400 W, incomplete evaporation of the ammonia refrigerant was found to occur due to a large fraction of water present in the solution. While the former result has some impact on the COP that can be obtained (greater sub-cooling prior to the evaporator is preferable for a higher COP), the system performance at present is dominated by the latter result, which significantly restricts the cooling output that can be achieved (the maximum cooling output of 104 W is some 13% below the "nominal" system output).

Further work will investigate first the effect of modifying the air-side characteristics of the evaporator, including the air flow-rate and the delivered cooling temperature. It is also expected that increasing the quantity of inert gas (hydrogen) in the system should lead to lower refrigerant partial pressures in the evaporator, thereby increasing the potential to achieve full evaporation. Adjustments to the thermodynamic model are also planned in order to more accurately describe the heat transfer processes in the evaporator and to account for incomplete evaporation, thus providing improved performance predictions at higher generator heat inputs.

ACKNOWLEDGEMETS

This work was supported by the UK Engineering and Physical Sciences Research Council (EPSRC) [grant numbers EP/P004709/1, EP/M025012/1 and EP/P030920/1]. Data supporting this publication can be obtained on request from cep-lab@imperial.ac.uk.

REFERENCES

[1] International Energy Agency, Energy Technology Perspectives 2016: Towards Sustainable Urban Energy Systems, OECD/IEA.

[2] Von Platen, B.C., Munters, C.G., US Patent. US 1685764 A. 1928.

[3] McCarney, S., Robertson, J., Arnaud, J., Lorenson, K., Lloyd, J., Using solar-powered refrigeration for vaccine storage where other sources of reliable electricity are inadequate or costly, *Vaccine*, Vol. 31, No. 51, 2013, pp. 6050-6057.

[4] Srikhirin, P., Aphornratana, S. and Chungpaibulpatana, S., A review of absorption refrigeration technologies, *Renewable and sustainable energy reviews*, Vol. 5, No. 4, 2001, pp. 343-372.

[5] Acuña, A., Velázquez, N., Sauceda, D., Rosales, P., Suastegui, A. and Ortiz, A., Influence of a compound parabolic concentrator in the performance of a solar diffusion absorption cooling system. *Applied Thermal Engineering*, Vol. 102, 2016, pp. 1374-1383.

[6] Schmid, F. and Spindler, K., Experimental investigation of the auxiliary gas circuit of a diffusion absorption chiller with natural and forced circulation, *International Journal of Refrigeration*, Vol. 70, 2016, pp. 84-92.

[7] Starace, G. and De Pascalis, L., An advanced analytical model of the Diffusion Absorption Refrigerator cycle, *International Journal of Refrigeration*, Vol. 35, 2012, pp. 605-612.

[8] Pátek, J. and Klomfar, J., Simple functions for fast calculations of selected thermodynamic properties of the ammonia-water system, *International Journal of Refrigeration*, Vol. 18 No. 4, 1995, pp. 228-234.

[9] Zohar, A., Jelinek, M., Levy, A. and Borde, I., 2005, Numerical investigation of a diffusion absorption refrigeration cycle, *International Journal of Refrigeration*, Vol. 28 No. 4, 2015, pp. 515-525.